J. Plasma Physics (2005), *vol.* 71, *part* 5, *pp.* 563–578. © 2005 Cambridge University Press
doi:10.1017/S0022377804003356 Printed in the United Kingdom

Electron beam–electromagnetic field interaction in one-dimensional coaxial vircator

H. SHAO, G. Z. LIU and Z. F. YANG

Northwest Institute of Nuclear Technology, PO Box 69-13, Xi'an, 710024, P. R. China
(shaohao@nint.ac.cn)

(Received 24 March 2004 and accepted 18 August 2004)

Abstract. A one-dimensional model of the interaction between an injected electron beam and an electromagnetic (EM) field inside a coaxial vircator is presented. The effects of the injected electron beam energy spread, anode absorption rate, feedback and injected current premodulation are analyzed. The EM-gains of interaction between the electron beam and TM_{01}, TE_{11} modes are derived and discussed.

1. Introduction

Research activities in the generation of high-power microwaves (HPMs) have been carried out by different research groups during last four decades. Many novel devices were designed, and these tested the availability of producing high-efficiency, long-duration and high-peak-power HPM pulses. The virtual cathode oscillator can meet all of the required characteristics of the ever-increasing demand of applications except it has low efficiency. Hence, most of the research efforts on the vircator are focused on peering into the physics of this device and searching for the new ways to improve the efficiency.

A coaxial vircator has been tested for its capability to generate HPM pulses with higher efficiency than other space-charge-effect devices without an external applied magnetic field. Although it is simple in configuration, the interaction between the electron beam and electromagnetic (EM) field inside the vircator system is very complicated. Many theoretical models were proposed to describe the physics of a vircator, but most of them are either without explicit form or without a clear physical picture of the mechanism of beam–EM field interaction.

In this paper, we try to give a simple theoretical analysis model of a coaxial vircator based on one-dimensional and quasi-steady-state hypotheses. Under these hypotheses, the interaction between the electron beam and EM field can be described as follows. The uniform electron beam is injected from the anode and moves to the virtual cathode. Here we do not care about the preliminary stage of the formation of the virtual cathode. It is just used as an existing boundary condition. If an oscillating radial electric field exists in the electron transit gap, it will cause a modulation of the electron distribution on the phase circle of the EM-field oscillation from uniformity to a bunch. Then the EM-field interacts with the bunched electron beam and results in the energy exchange.

https://doi.org/10.1017/S0022377804003356 Published online by Cambridge University Press

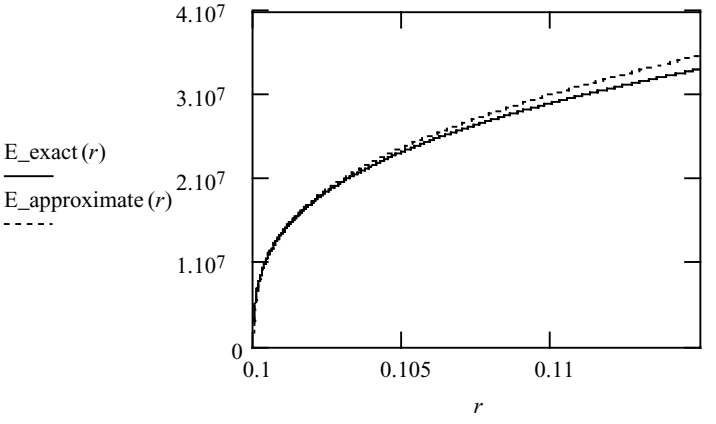


Figure 1. Electric-field distribution versus r in a coaxial vircator.

2. Electric-field distribution inside a one-dimensional coaxial vircator

The virtual cathode formed inside a coaxial vircator is caused by the space charge of the injected electron beam, so the electric-field distribution generated by the beam charge can be obtained by a Poisson equation,

$$\frac{1}{r}\frac{\partial}{\partial r}(r \cdot E) = \frac{\rho}{\varepsilon_0}, \tag{1}$$

where E, ρ, ε_0 are the electric field, charge density and free space permittivity.

Based on Maxwell's equation, we have

$$\nabla \times B = \mu_0 J + \mu_0 \varepsilon_0 \frac{\partial E}{\partial t}, \tag{2}$$

where B, μ_0, J are the magnetic field, free space permeability and current density. Since we consider a quasi-steady-state electron beam flow, namely, $\partial E/\partial t = 0$, deriving the divergence of (2) gives

$$J = \frac{I_0}{2\pi r}, \tag{3}$$

where I_0 is the axial current per unit length.

Substituting $J = -nev$, $\rho = -ne$ and (3) into (1), and solving with boundary condition $E(r = r_{\mathrm{vco}}) = 0$, the electric field is approximately given as a function of relativistic factor γ,

$$E(r) \simeq \left(\frac{I_0 mc}{\pi \varepsilon_0 e}\right)^{1/2} [\gamma(r)^2 - 1]^{1/4} r^{-1/2} \tag{4}$$

here n, e, v are respectively electron density, charge and velocity.

Using a set of practical parameters (500 kV diode voltage, 250 A cm^{-2} current density on the anode and an anode radius of approximately 11 cm), we can obtain the numerical results of (1) and (4) as shown in Fig. 1.

From Fig. 1 we can see that the two curves behave the same and give almost the same value with the variation of r. The maximal deviation of (4) from (1) is no more than 10%. Therefore, we can conveniently use (4) in the following theoretical

https://doi.org/10.1017/S0022377804003356 Published online by Cambridge University Press

analysis process without introducing any relatively large deviation from the exact value.

Considering that an electron moves from the virtual cathode to the anode, we have

$$dt = \frac{dr}{v} = -\frac{2\pi\varepsilon_0}{I_0} d(rE). \tag{5}$$

Integrating (5) we can obtain the electron transit-time ($\bar{\tau}$) from the virtual cathode to the anode

$$\bar{\tau} = \left(\frac{2\varepsilon_0 m\gamma_0}{e^2 n_0}\right)^{1/2} = \frac{\sqrt{2}}{\omega_\mathrm{p}} \tag{6}$$

with ω_p the plasma frequency given by

$$\omega_\mathrm{p} = \left(\frac{n_0 e^2}{\varepsilon_0 m\gamma_0}\right)^{1/2}. \tag{7}$$

Equation (6) is the same as that obtained from a planar vircator [1], which implies that the coaxial vircator acts in somewhat the same way as the planar vircator.

3. Resonance between injected electrons and an oscillating electric field

Supposing an oscillating electric field applied inside the anode cylinder, it must be present as the EM-field component of a certain cylindrical waveguide mode. In most cases, the coaxial vircator works with the lowest two modes—TM_{01} and TE_{11}—hence, the following theoretical derivations are based on these two basic modes.

First, we consider the interaction between injected electrons and the TM_{01} mode. The radial electric-field component of the TM_{01} mode is given by

$$E_\mathrm{ext}(r,t) = E_1(r)E_2(t) = E_1(r)\sin\beta z \sin\omega t, \tag{8}$$

with

$$E_1(r) = J_1\left(2.405\frac{r}{r_0}\right) E_{\mathrm{ext0-TM_{01}}},$$

r_0 the anode radius, J_1 the first-order Bessel function, E_ext0 the electric-field amplitude and ω the oscillation frequency. The axial length of the electron injecting region is generally comparatively smaller than the guide wavelength. For simplicity, the electric field can use the maximal value; that is, $\sin\beta z = 1$.

Consider an electron with momentum p_0 injected at time $t = t_0$ from the anode position, the momentum decreases as it approaches the virtual cathode, and at the time $t = t_0 + \tau_1$ it reaches 0. Then we have [1–3]

$$p_0 = \frac{1}{r_\mathrm{vco} - r_0}\int_{r_0}^{r_\mathrm{vco}}\int_{t_0}^{t_0+\tau_1} e[E_\mathrm{self}(r,t) + E_\mathrm{ext}(r,t)]\,dt\,dr, \tag{9}$$

here $E_\mathrm{self}(r,t)$ is the electric field generated by the electron space charge, and under a quasi-steady-state hypothesis it becomes $E_\mathrm{self}(r)$. The boundary condition here is $dE_\mathrm{self}(r)/dr|_{r=r_\mathrm{vco}} = 0$. $E_\mathrm{ext}(r,t)$ is the oscillating electric field given by (8). After that, the electron returns to the anode with time duration τ_2, and the momentum

https://doi.org/10.1017/S0022377804003356 Published online by Cambridge University Press

reaches p, which gives

$$p = \frac{1}{r_0 - r_{\rm vco}} \int_{r_{\rm vco}}^{r_0} \int_{t_0+\tau_1}^{t_0+\tau_1+\tau_2} e[E_{\rm self}(r) + E_{\rm ext}(r,t)]\, dt\, dr. \tag{10}$$

Using the same derivation methods as used in [1], the average electron momentum loss, namely the EM-field gain as a result of the interaction between the electron beam and oscillating electric field in one oscillation period, is given by

$$G = \overline{\left(\frac{p_0 - p}{p_0}\right)} = \frac{4eKE_{\rm ext0-TM_{01}}}{\omega T p_0 (r_{\rm vco} - r_0)} \int_0^T \left[\sin^2 \frac{\omega(\bar{\tau} + \Delta)}{2} \cos\omega(t_0 + \bar{\tau} + \Delta)\right] dt_0, \tag{11}$$

where

$$K = \frac{r_0}{2.405} J_0\left(2.405 \frac{r_{\rm vco}}{r_0}\right),$$

J_0 is zero Bessel function. Here we also introduce the concept of a transit time shift: $\Delta = \tau - \bar{\tau}$ with $\tau = \tau_1 = \tau_2$ the transit time and $\bar{\tau}$ the average transit time, according to which the electron phase shift in half an oscillating period is

$$\omega\Delta \simeq -\frac{2E_{\rm ext0-TM_{01}}}{V_0/K} \sin\omega\left(t_0 + \frac{\bar{\tau}}{2}\right) \sin\frac{\omega\bar{\tau}}{2}. \tag{12}$$

From (11) we can see that if it is positive, the electron will give out energy to the EM-field inside the anode cylinder, and the electron will gain energy from the EM-field when it is negative.

Substitute (12) into (11), the EM-field gain (average electron momentum loss) is obtained as

$$G = \overline{\left(\frac{p_0 - p}{p_0}\right)} = -\frac{2A}{s\pi} \int_0^{2\pi} \left\{\sin^2\left[\frac{s}{2} - A\sin\frac{s}{2}\sin\left(\theta + \frac{s}{2}\right)\right] \times \cos\left[\theta + s - 2A\sin\frac{s}{2}\sin\left(\theta + \frac{s}{2}\right)\right]\right\} d\theta, \tag{13}$$

where

$$A = \frac{E_{\rm ext0-TM_{01}}}{V_0/K}$$

is the ratio of the oscillating electric-field amplitude, $E_{\rm ext0}$, and normalized space charge electric field, V_0/K, $s = \omega\bar{\tau}$, $\theta = \omega t_0$.

Using the same parameters as used in calculating Fig. 1, the EM-field gain as a function of normalized frequency, $\omega/\omega_{\rm p}$, is given in Fig. 2 from (13).

Figure 2 shows that under many frequency bands, the EM-field gain can be positive, and it is sensitive to the ratio of the oscillating electric-field amplitude and normalized space charge electric field. The EM-field gain reaches its maximum around $\omega/\omega_{\rm p} = 2.9$ in the first positive value frequency band.

Here, $\omega/\omega_{\rm p} = 2.9$ is used in calculating EM-field gain as a function of A from (13), as shown in Fig. 3. It shows that the EM-gain increases sharply with the electric-field ratio A from zero and reaches a maximum at about 0.86. As A increases, it has another peak value at about 2.27. This indicates that the electron phase shift caused by the oscillating electric field which is overdue when A is greater than 0.86 and which will lead to some bunches of electrons, is on the wrong phase of electric field and obtains energy, and thus finally results in a decrease in the overall EM-field gain.

https://doi.org/10.1017/S0022377804003356 Published online by Cambridge University Press

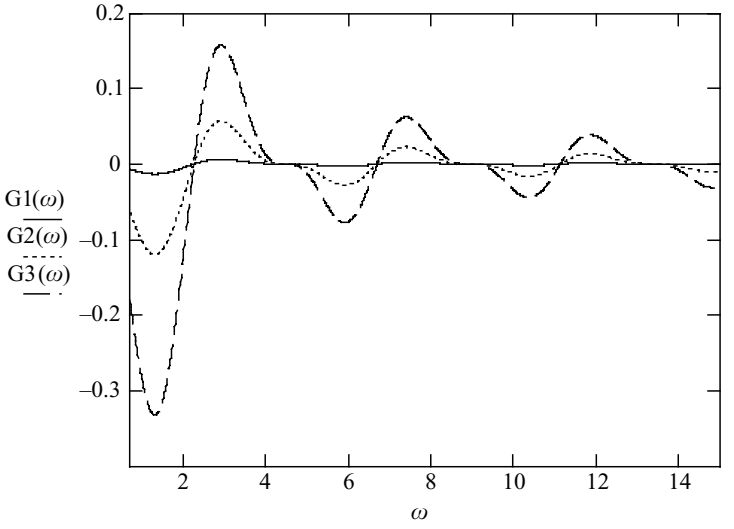


Figure 2. EM-field gain as a function of normalized frequency. G1: $A = 0.1$; G2: $A = 0.3$; G3: $A = 0.5$.

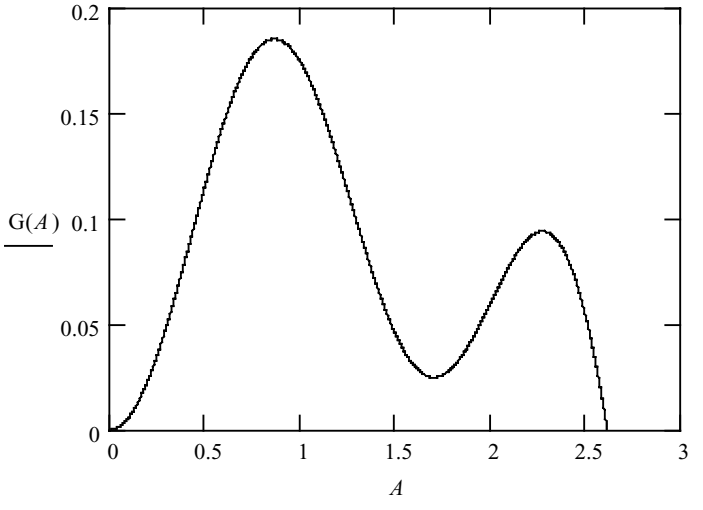


Figure 3. EM-field gain as a function of electric-field ratio A.

The relation between the EM-field gain and system energy efficiency can be approximately given by

$$G = \overline{\left(\frac{p_0 - p_1}{p_0}\right)} \simeq \frac{\sqrt{2\gamma_0 m_0 E_0} - \sqrt{2\gamma_0 m_0 E_1}}{\sqrt{2\gamma_0 m_0 E_0}}, \tag{14}$$

where E_0 is electron initial energy, and E_1 is electron energy after one period of interaction with electric field. From (14), the electron energy gain after one

https://doi.org/10.1017/S0022377804003356 Published online by Cambridge University Press

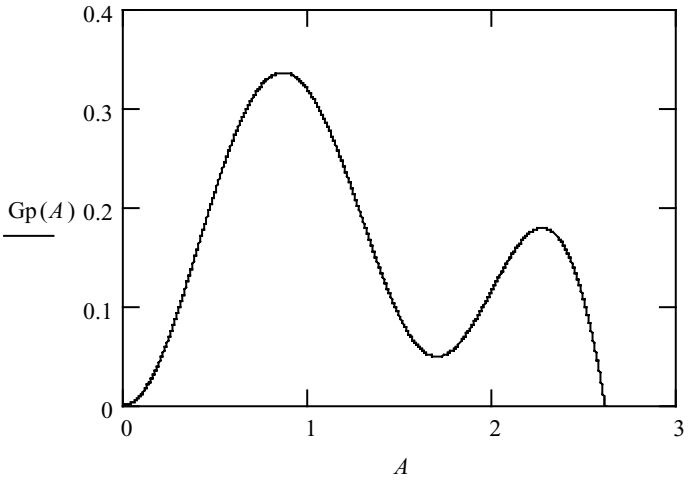


Figure 4. Power efficiency versus A.

interaction circle (in other words the power efficiency) can be derived as

$$G_{\mathrm{p}} = \overline{\left(\frac{E_0 - E_1}{E_0}\right)} = 1 - [1 - G]^2 . \tag{15}$$

According to (15), Fig. 3 can be converted into power efficiency versus A as shown in Fig. 4.

From Fig. 4 we can see that, theoretically, the power efficiency of a coaxial vircator can be more than 30% when the oscillating electric field has an amplitude nearly the same as that of the normalized space charge generated electric field. Hence, for achieving high efficiency in a coaxial vircator, it is vital to enhance the amplitude of the oscillating electric field by introducing feedback or other methods.

4. Effect of the initial momentum spread of the injected electron beam on the EM-field gain

Until now, all the derivations are based on the uniform momentum of injected electrons. If there is a momentum spread in the injected electron beam, it will affect the beam–EM-wave interaction, and results in an extra phase shift of electron bunches. Therefore, this effect must be taken into account when considering the system efficiency.

Set the constant current of the injected electron beam, but with a momentum spread as a Gaussian distribution in the region between $p_0 - p_1$ and $p_0 + p_1$, the probability distribution function is

$$f(x) = \frac{1}{\sqrt{2\pi}(p_1/3)} \exp\left[-\frac{(x - p_0)^2}{2(p_1/3)^2}\right] . \tag{16}$$

Supposing the momentum variation from p_0 to $p_0 + p_1$ causes a deviation in the electron transit time δ, and we have

$$\omega\delta = \sqrt{2}\frac{p_1}{p_0}\frac{\omega}{\omega_{\mathrm{p}}}. \tag{17}$$

https://doi.org/10.1017/S0022377804003356 Published online by Cambridge University Press

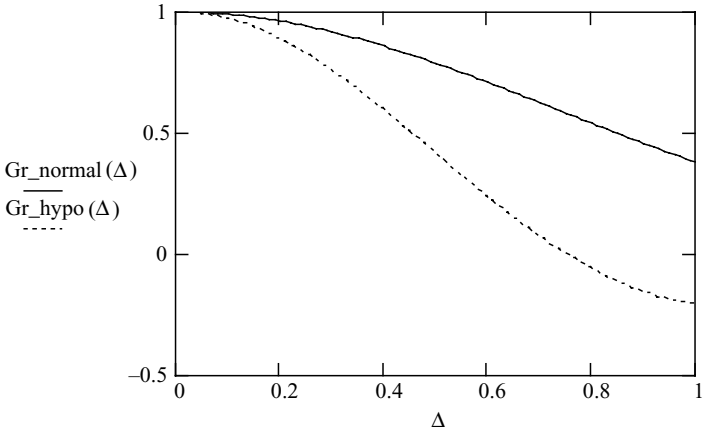


Figure 5. EM-gain ratio as a function of momentum spread Δ, where $\Delta = p_1/p_0$.

Substitute (16), (17) into (13) and taking into account the electrons injected from $t_0 - \delta$ to $t_0 + \delta$ to obtain,

$$G_{\text{normal}} = \overline{\left(\frac{p_0 - p}{p_0}\right)} = -\frac{2A}{s\pi}\int_0^{2\pi}\left\{\sin^2\left[\frac{s}{2} - A\sin\frac{s}{2}\sin\left(\theta + \frac{s}{2}\right)\right]\right.$$
$$\times \int_{\theta-\omega\delta}^{\theta+\omega\delta}\frac{1}{\sqrt{2\pi}(\omega\delta/3)}\exp\left[-\frac{(\beta-\theta)^2}{2(\omega\sigma/3)^2}\right]$$
$$\left.\times\cos\left[\beta + s - 2A\sin\frac{s}{2}\sin\left(\theta + \frac{s}{2}\right)\right]d\beta\right\}d\theta. \tag{18}$$

Meanwhile, for simplicity, we can also set a uniform distribution of momentum spread, which gives the EM gain as

$$G_{\text{hypo}} = \overline{\left(\frac{p_0 - p}{p_0}\right)} = -\frac{2A}{s\pi}\frac{\sin\omega\delta}{\omega\delta}\int_0^{2\pi}\left\{\sin^2\left[\frac{s}{2} - A\sin\frac{s}{2}\sin\left(\theta + \frac{s}{2}\right)\right]\right.$$
$$\left.\times\cos\left[\theta + s - 2A\sin\frac{s}{2}\sin\left(\theta + \frac{s}{2}\right)\right]\right\}d\theta. \tag{19}$$

(13) Divided by (18) and (19), we can obtain the EM-gain ratios G_{normal}/G and G_{hypo}/G as shown in Fig. 5.

The curves in Fig. 5 indicate that in the range of 20% momentum spread, the EM gain is almost unaffected by the Gaussian distribution of the momentum spread. In plasma physics, the particle physical parameters distribution generally agrees with Gaussian distribution, therefore it is closer to the real case than that of the uniform distribution [2, 4].

5. Effect of the anode absorption rate on EM-field gain

Previously, we have assumed that the electrons are absorbed when they return to the anode after one interaction circle. In fact, most returned electrons will re-enter the diode gap and then again be accelerated by the diode electric field. In this case, the residual energy of the reflected electrons can be recycled depending on the

https://doi.org/10.1017/S0022377804003356 Published online by Cambridge University Press

circles before it is absorbed by the anode. Meanwhile, the circulation of reflected electrons also introduces momentum spread to the injected electron beam.

Under the one-dimensional hypothesis, the electron only moves along radial direction, so it can only be absorbed by the anode. Suppose that the anode has an absorption rate of ζ, in other words, the probability of being absorbed is ζ when a electron passes through the anode. When the absorbtion probability approaches 99%, we say it is absorbed. Before the electron is absorbed, the number of cycles k is given the name of electron life cycles. In one cycle, the electron passes through the anode twice. Then, we have

$$(1-\zeta)^{2k} = 0.01. \tag{20}$$

Solving (20) gives

$$k = -\frac{1}{\log(1-\zeta)}. \tag{21}$$

The number of life cycles of electrons is k, namely every electron interacts k times with EM field. Consequently, the EM gain here should be multiplied by k. On the other hand, electron recycling will bring the momentum spread due to every interaction causing it to lose energy. Suppose that the injecting current remains constant, on average, then only $1/k$ of the injected electrons are newly produced with momentum p_0. Other electrons are recycled and their momentums depend on their recycling times. Assuming that one interaction causes a momentum loss of p_2, then k electron life cycles will approximately cause a momentum loss of kp_2, from which we have overall momentum spread as

$$p_1 = \left(1-\frac{1}{k}\right)\left[\sum_{i=1}^{\infty}\left(\frac{1}{k}\right)^{i-1}(i-1)\right]p_2 = (k-1)\,p_2. \tag{22}$$

According to (13), the momentum loss p_2 caused by one time interaction can be given by

$$p_2 = G(A)p_0. \tag{23}$$

Substituting (23) into (22) gives

$$p_1/p_0 = (k-1)G(A). \tag{24}$$

For simplicity, suppose that the energy spread is in uniform distribution, substituting (24) into (19) and dividing it by (13), we have

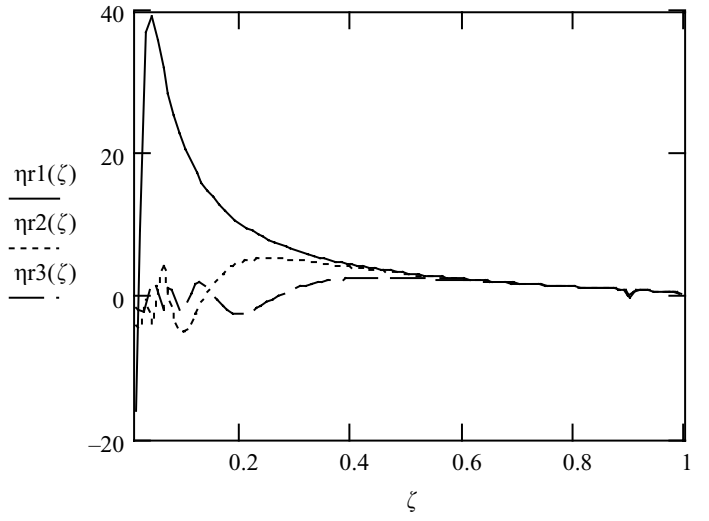
$$\frac{\eta}{\eta_0} = k\frac{\sin[\sqrt{2}(k-1)G(\omega/\omega_{\mathrm{p}})]}{\sqrt{2}(k-1)G(\omega/\omega_{\mathrm{p}})}. \tag{25}$$

The relation between the anode absorption efficiency and EM gain can be obtained by substituting (21) into (25), which gives

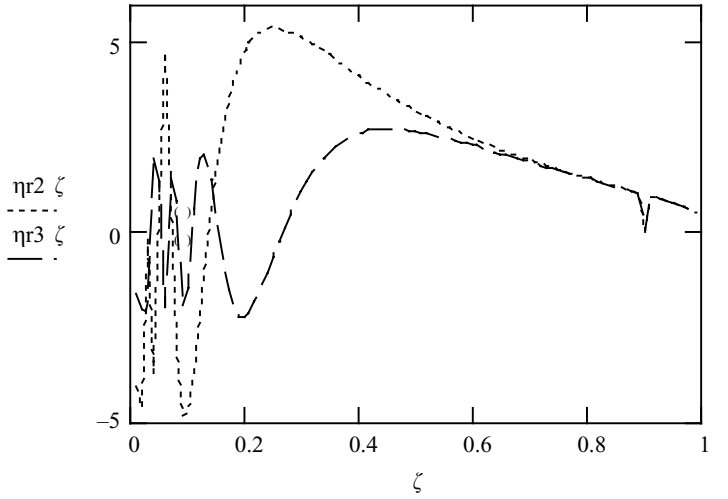
$$\frac{\eta}{\eta_0} = -\frac{1}{\log(1-\zeta)}\frac{\sin[\sqrt{2}(1/\log(1-\zeta)+1)G(A)(\omega/\omega_{\mathrm{p}})]}{\sqrt{2}(1/\log(1-\zeta)+1)G(A)(\omega/\omega_{\mathrm{p}})}. \tag{26}$$

Equation (26) is schematically visualized in Fig. 6. It indicates that the EM-gain enhancement resulting from electron recycling is susceptive to the value of A. Under a small electric-field ratio, the EM gain increases sharply with increasing recycling times, whereas when A is large, too many electrons recycling will lead to a decrease in EM gain. Meanwhile, decreasing the anode absorption rate can help

https://doi.org/10.1017/S0022377804003356 Published online by Cambridge University Press



(a)



(b)

Figure 6. EM gains versus a node absorption rate. ηr1: $A = 0.1$; ηr2: $A = 0.3$; ηr3: $A = 0.5$.

improve EM gain to a certain extent, but the effect of anode absorption efficiency on EM gain is not monotonic, which agrees with previous simulation results [5].

6. Effect of feedback on power efficiency

Figure 3 denotes that if we can increase the oscillating electric field to the level of the space charge generated electric field, the power efficiency of the coaxial vircator will reach as high as 30%. There are many ways to increase the level of oscillating electric field in the interaction region. One of the easiest ways is to introduce output power feedback.

https://doi.org/10.1017/S0022377804003356 Published online by Cambridge University Press

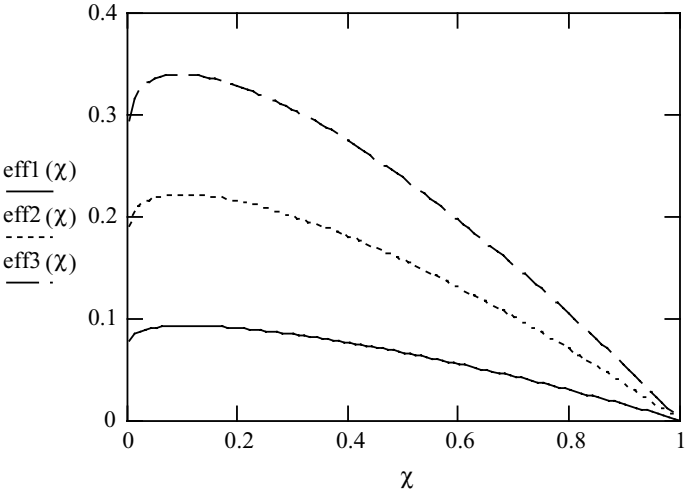


Figure 7. Power efficiency as a function of feedback coefficient. eff1: $G_0 = 0.04$, eff2: $G_0 = 0.1$, eff3: $G_0 = 0.16$.

For effectively increasing the amplitude of the oscillating electric field, it is required that the feedback EM field must be in-phase with the existing oscillating electric field inside the interaction region, which can be easily achieved by adjusting the feedback position. The electric field in the output region is kept at the same level as that in the interaction region under the quasi-steady-state hypothesis. Set the feedback coefficient, namely the power reflection coefficient χ from (15), and the power efficiency is now given by

$$G_{\text{power}} = \{1 - [1 - G]^2\}(1 - \chi). \tag{27}$$

The amplitude of the electric field in the interaction region becomes $(1 + \sqrt{\chi})E_{\text{ext0}}$, substituting it into (13) gives

$$G_1 = (1 + \sqrt{\chi})G_0 \tag{28}$$

where G_1, G_0 are, respectively, the EM gain with and without feedback. Substituting this into (27), we have

$$G_{\text{power}} = \{1 - [1 - (1 + \sqrt{\chi})G_0]^2\}(1 - \chi). \tag{29}$$

Figure 7 indicates that introducing feedback in coaxial vircator can slightly improve power efficiency, and the efficiency reaches a maximal value at $\chi \approx 0.1$. Then, it decreases with increasing χ.

7. Effect of premodulation of the injected beam current on efficiency

Suppose a premodulation applied on the injected electron beam current. To resonate with the oscillating electric field in the interaction region, it must bear the same or be near the frequency of the electric field. Consequently, under the quasi-steady-state hypothesis, the injected current per unit length along the axial direction can be written as

$$I_{\text{in}} = I_0[1 + \xi \sin(\omega t + \theta_0)], \tag{30}$$

https://doi.org/10.1017/S0022377804003356 Published online by Cambridge University Press

where I_0 is the time-averaged value of the injected current, ξ is the premodulation amplitude, θ_0 is the initial phase of premodulation. Substituting (30) into (4), the space charge generated electric field in the interaction region is given as

$$E_{\text{self}}(r,t) \simeq E_0(r)[1+\xi\sin(\omega t+\theta_0)]^{1/2} \tag{31}$$

with

$$E_0(r) = \left(\frac{I_0 mc}{\pi\varepsilon_0 e}\right)^{1/2}(\gamma^2-1)^{1/4}r^{-1/2}.$$

Since the average momentum of injected electrons is still p_0, (9) is still valid in this case. Also, according to the same derivation methods as used in [1, 6], the EM gain here is obtained as

$$\begin{aligned} G &= \overline{\left(\frac{p_0-p}{p_0}\right)} \\ &= \frac{e}{Tp_0(r_{\text{vco}}-r_0)}\int_0^T\left\langle\int_{r_0}^{r_{\text{vco}}}\left\{\int_{t_0}^{t_0+\tau}E_{\text{self}}(r,t)\,dt-\int_{t_0+\tau}^{t_0+2\tau}E_{\text{self}}(r,t)\,dt\right.\right. \\ &\quad\left.\left.+\int_{t_0}^{t_0+\tau}E_{\text{ext}}(r,t)\,dt-\int_{t_0+\tau}^{t_0+2\tau}E_{\text{ext}}(r,t)\,dt\right\}dr\right\rangle dt_0. \end{aligned} \tag{32}$$

Substituting (31) and (8) into (32), we have

$$\begin{aligned} G &= \overline{\left(\frac{p_0-p}{p_0}\right)} \\ &= \frac{e}{Tp_0(r_{\text{vco}}-r_0)}\int_0^T\left\langle\int_{r_0}^{r_{\text{vco}}}E_0(r)\,dr\left\{\int_{t_0}^{t_0+\tau}[1+\xi\sin(\omega t+\theta_0)]^{1/2}\,dt\right.\right. \\ &\quad\left.\left.-\int_{t_0+\tau}^{t_0+2\tau}[1+\xi\sin(\omega t+\theta_0)]^{1/2}\,dt\right\}\right\rangle dt_0 \qquad (33a) \\ &\quad+\frac{e}{Tp_0(r_{\text{vco}}-r_0)}\int_0^T\left\{\int_{r_0}^{r_{\text{vco}}}E_1(r)\,dr\right. \\ &\quad\left.\times\left(\int_{t_0}^{t_0+\tau}\sin\omega t\,dt-\int_{t_0+\tau}^{t_0+2\tau}\sin\omega t\,dt\right)\right\}dt_0. \qquad (33b) \end{aligned}$$

Equation (33) can be divided into two items, the first item (33a) represents the EM gain results from the injected current premodulation, and the second which results from the oscillating electric field. Hence, the second item (33b) has the same form as (11), namely,

$$(33\text{b}) = \frac{4e}{\omega Tp_0(r_{\text{vco}}-r_0)}K\cdot E_{\text{ext0}}\int_0^T\left[\sin^2\frac{\omega(\bar{\tau}+\Delta)}{2}\cos\omega(t_0+\bar{\tau}+\Delta)\right]dt_0 \tag{34}$$

https://doi.org/10.1017/S0022377804003356 Published online by Cambridge University Press

and the first item can be written in simple form as

$$(33a) = -\frac{eV_0}{Tp_0(r_{vco}-r_0)}\int_0^T \left\{ \int_{t_0}^{t_0+\tau} [1+\xi\sin(\omega t+\theta_0)]^{1/2}\,dt - \int_{t_0+\tau}^{t_0+2\tau} [1+\xi\sin(\omega t+\theta_0)]^{1/2}\,dt \right\} dt_0. \tag{35}$$

Introducing the electron transit time deviation $\Delta = \tau - \bar{\tau}$ and using the same methods as deviating (13), (34) and (35) become

$$(34) = -\frac{2A}{s\pi}\int_0^{2\pi} \left\{ \sin^2\left[\frac{s}{2} - A\sin\frac{s}{2}\sin\left(\theta+\frac{s}{2}\right)\right] \times \cos\left[\theta + s - 2A\sin\frac{s}{2}\sin\left(\theta+\frac{s}{2}\right)\right]\right\} d\theta \tag{36}$$

$$\begin{aligned}(35) = {} & \frac{1}{2\pi s}\int_0^{2\pi} \left\{ \int_{\theta}^{\theta-2A\sin(\theta+s/2)\sin(s/2)+s} \left[1+\frac{\xi}{2}\sin(\alpha+\theta_0) - \frac{\xi^2}{8}\sin^2(\alpha+\theta_0) + \frac{\xi^3}{16}\sin^3(\alpha+\theta_0) + \mathrm{L}\right] d\alpha \right. \\ & \left. - \int_{\theta-2A\sin(\theta+s/2)\sin(s/2)+s}^{\theta-4A\sin(\theta+s/2)\sin(s/2)+2s} \left[1+\frac{\xi}{2}\sin(\alpha+\theta_0) - \frac{\xi^2}{8}\sin^2(\alpha+\theta_0) + \frac{\xi^3}{16}\sin^3(\alpha+\theta_0) + \mathrm{L}\right] d\alpha \right\} d\theta \\ = {} & -\frac{2\xi}{s\pi}\int_0^{2\pi} \left\{ \sin^2\left[\frac{s}{2} - A\sin\left(\theta+\frac{s}{2}\right)\sin\frac{s}{2}\right] \times \cos\left[\theta - 2A\sin\left(\theta+\frac{s}{2}\right)\sin\frac{s}{2} + s + \theta_0\right] + \mathrm{L}\right\} d\theta. \end{aligned} \tag{37}$$

The EM gains with premodulation of the injected electron beam current according to (36) and (37) are shown in Fig. 8. It indicates that the premodulation can effectively improve the EM gains, and the initial phase of premodulation periodically affects the efficiency. The maximal EM gains are presented at

$$\theta_{0-\max} \approx 2\pi i + 0.61, \quad i = 0, 1, 2 \ldots, n. \tag{38}$$

Figure 9 gives the EM gain as a function of premodulation amplitude ξ, which indicates, within the frequency band where EM gain is positive, that it increases almost linearly with ξ.

8. Electron beam resonance with the electric field of the TE_{11} mode

Since the TE_{11} mode is the lowest mode in a circular waveguide, in many cases we have to take into account the effect of electron beam resonance with the electric-field component of it. Meanwhile, the TE_{11} mode have the most intensive radial electric field, therefore it is expected to have a high coupling coefficient with the radial injected electron beam.

https://doi.org/10.1017/S0022377804003356 Published online by Cambridge University Press

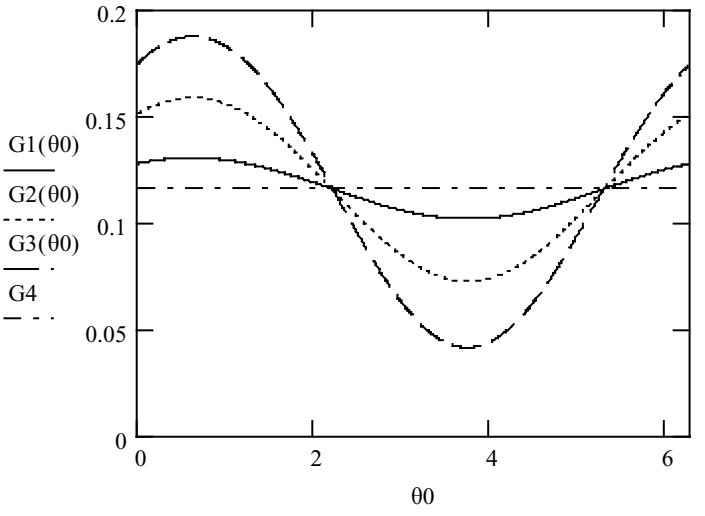


Figure 8. EM gains versus initial phase of injected current premodulation. G1: $A = 0.1$, G2: $A = 0.3$, G3: $A = 0.5$, G4: $A = 0$.

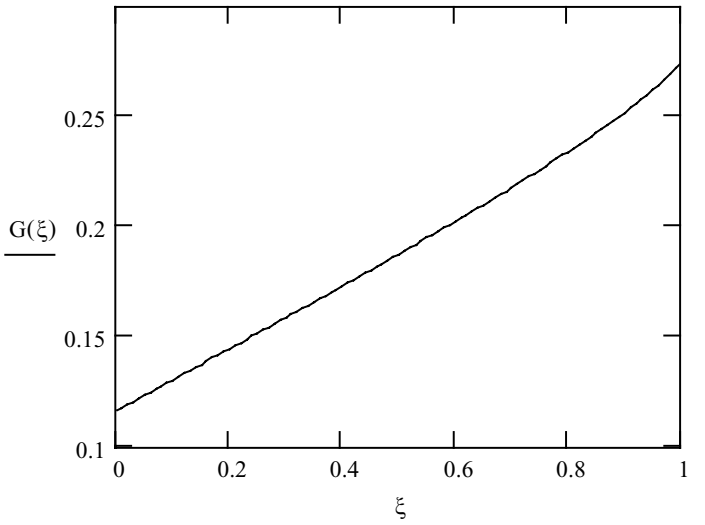


Figure 9. EM gain as a function of premodulation amplitude ξ.

Here we still adopt the model of azimuthally uniform injected current. According to the mode character of TE_{11}, the interaction between this mode and the injected electron beam will result in the electrons injected from circular symmetry directions being in reverse phase. The radial electric-field component of TE_{11} modes is given by

$$E_{\text{ext}} = E_{\text{ext0}-\text{TE}_{11}} E_{\text{TE}_{11}}(r) \sin\varphi \sin\beta z \sin\omega t \tag{39}$$

with

$$E_{\text{TE}_{11}}(r) = \frac{r_0}{r} J_1\left(\frac{1.841}{r_0} r\right)$$

https://doi.org/10.1017/S0022377804003356 Published online by Cambridge University Press

and the same simplification as in Sec. 2, $\sin\beta z \simeq 1$. From (9) and (10) we obtain the EM gain of the interaction between the TE_{11} mode and injected electron beam as

$$\overline{\left(\frac{p_0-p}{p_0}\right)} = \frac{e}{Tp_0(r_{\text{vco}}-r_0)}\int_0^T \left\langle \int_{r_0}^{r_{\text{vco}}} \left\{ \int_{t_0}^{t_0+\tau_1} \left[E_{\text{self}}(r) + \frac{\int_0^\pi E_{\text{ext}}(r,t)\,d\varphi}{\pi} \right] dt \right.\right.$$
$$\left.\left. - \int_{t_0+\tau_1}^{t_0+\tau_1+\tau_2} \left[E_{\text{self}}(r) + \frac{\int_0^\pi E_{\text{ext}}(r,t)\,d\varphi}{\pi} \right] dt \right\} dr \right\rangle dt_0. \tag{40}$$

Taking the same process of derivation as used in Sec. 2, (40) is reduced to

$$\overline{\left(\frac{p_0-p}{p_0}\right)} = \frac{8eE_{\text{ext0-TE}_{11}}K}{\omega\pi Tp_0(r_{\text{vco}}-r_0)}\int_0^T \sin^2\frac{\omega(\bar\tau+\Delta)}{2}\cos\omega(t_0+\bar\tau+\Delta)\,dt_0, \tag{41}$$

where

$$K = -\int_{r_0}^{r_{\text{vco}}} \frac{r_0}{r} J_1\left(\frac{1.841}{r_0}r\right) dr,$$

and $\bar\tau$, Δ have the same forms as in (13).

The electron phase shift within a half period is

$$\omega\Delta \simeq \frac{4A}{\pi}\sin\omega\left(t_0+\frac{\bar\tau}{2}\right)\sin\frac{\omega\bar\tau}{2}. \tag{42}$$

where $A = E_{\text{ext0-TE}_{11}}/(V_0/K)$.

Substituting (42) into (41) gives the EM gain as

$$G_{l-\text{TE}_{11}} = \overline{\left(\frac{p_0-p}{p_0}\right)} = -\frac{4A}{\pi^2 s}\int_0^{2\pi} \left\{ \sin^2\left[\frac{s}{2} - \frac{2A}{\pi}\sin\left(\theta+\frac{s}{2}\right)\sin\frac{s}{2}\right] \right.$$
$$\left. \times \cos\left[\theta + s - \frac{4A}{\pi}\sin\left(\theta+\frac{s}{2}\right)\sin\frac{s}{2}\right] \right\} d\theta. \tag{43}$$

Comparing with (13), we find that the EM gains of resonance between TE_{11} or TM_{01} modes with oscillating electric field have almost the same form except for the amplitude.

Normalizing the average radial azimuthal electric field of TE_{11} and TM_{01} modes at the anode in (8) and (39), we have

$$J_1(2.405)E_{\text{ext0-TM}_{01}} = \frac{2}{\pi}J_1(1.841)E_{\text{ext0-TE}_{11}} \tag{44}$$

that can be reduced to the form

$$E_{\text{ext0-TE}_{11}}/E_{\text{ext0-TM}_{01}} = 1.401. \tag{45}$$

Accordingly, the normalized EM gain from resonance of the TE_{11} mode with oscillating electric field should be multiplied by 1.401. The comparison results are shown in Fig. 10.

It is shown in Fig. 10 that under a normalized oscillating electric field, the maximal EM-gain for these two types of mode has almost the same amplitude. So

https://doi.org/10.1017/S0022377804003356 Published online by Cambridge University Press

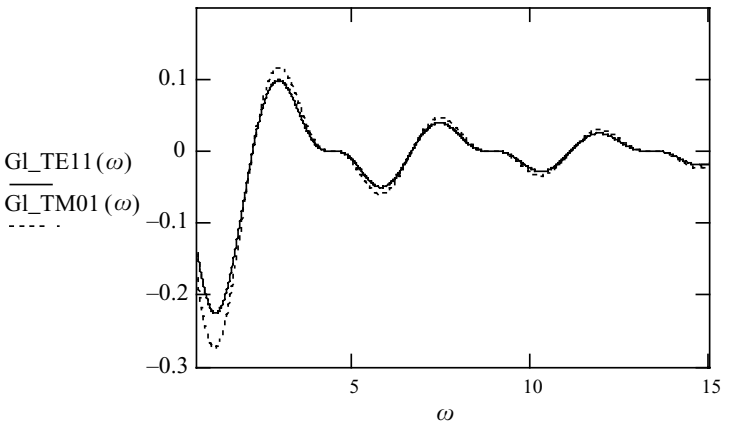


Figure 10. Normalized EM gains of resonance between the TM_{01}, TE_{11} modes and the oscillating electric field versus normalized frequency.

this means that the role of the TE_{11} mode's interaction with the oscillating electric field could not be neglected when considering the mechanism of a coaxial vircator. Moreover, since the TE_{11} mode is the basic mode in a circular waveguide and has the most intense radial electric-field component compared with other modes, the modes competition will enhance the TE_{11} component in overall EM power [6]. Meanwhile, any uncoaxiality between the anode and cathode results from system machining, and assembly will lead to non-uniform electron emission, which is usually present as a unipolar emission enhancement. In this case, the electron beam track is closer to the radial electric-field distribution of the TE_{11} mode. Hence, it is expected that the coupling coefficient between the TE_{11} mode and injected electron beam will increase.

9. Conclusions

Based on one-dimensional theoretical analysis, a coaxial vircator exhibits positive EM gain under a series of frequency bands. The maximum is present in the first band. Theoretically, the power efficiency of a coaxial vircator can reach more than 30%. The EM-gain is sensitive to the ratio between the oscillating electric-field amplitude and the normalized space-charge electric field. Increasing the oscillating electric-field amplitude to the level of the space-charge generated electric-field can effectively improve the energy conversion efficiency. The power efficiency of a coaxial vircator is not affected by an injected electron beam momentum spread within 20%. Decreasing the anode absorption rate can help improve EM gain, but its effect is not monotonic. Introducing feedback into the coaxial vircator can increase the power efficiency with the optimal reflecting coefficient. The injected beam current premodulation with proper initial phase can also effectively improve EM gain. Finally, under a normalized electric-field ratio, the TE_{11} and TM_{01} modes have almost the same EM gains. Hence, the effect of interaction between the TE_{11} mode and electron beam cannot be neglected in considering the overall efficiency of a coaxial vircator.

https://doi.org/10.1017/S0022377804003356 Published online by Cambridge University Press

References

[1] Jiang, W. and Kristiansen, M. 2001 *Phys. Plasma* **8**(8), 1.
[2] Sullivan, D. J., Walsh, J. E. and Coutsias, E. A. 1987 *High Power Microwave Sources* (ed. V. Granastein and L. Alexeff). Norwood, MA: Artech House, p. 441.
[3] Kadish, A., Faehl, R. J. and Snell, C. M. 1986 *Phys. Fluid* **29**(12), 4192.
[4] Greedon, J. M. 1975 *J. Appl. Physics* **46**(7), 2946.
[5] Shao, H. and Liu, G. Z. 2001 *Acta Phys. Sinica* **50**(12), 2387.
[6] Jiang, W., Masugata, K. and Yatsui, K. 1995 *Phys. Plasma* **2**(3), 982.

https://doi.org/10.1017/S0022377804003356 Published online by Cambridge University Press